Inorg. Chem. **2006**, *45*, 6269–6275

Formation and Reactivity of Ir(III) Hydroxycarbonyl Complexes

Paul I. P. Elliott,† Claire E. Haslam, Sharon E. Spey, and Anthony Haynes*

Department of Chemistry, University of Sheffield, Sheffield, S3 7HF, U.K.

Received February 1, 2006

Kinetic studies show that the reaction of $[TpIr(CO)_2]$ (**1**, Tp = hydrotris(pyrazolyl)borate) with water to give $[TpIr(CO_2H)(CO)H]$ (**2**) is second order ($k = 1.65 \times 10^{-4}$ dm^3 mol^{-1} s^{-1}, 25 °C, MeCN) with activation parameters $\Delta H^{\ddagger} = 46\pm2$ kJ mol^{-1} and $\Delta S^{\ddagger} = -162\pm5$ J K^{-1} mol^{-1}. A kinetic isotope effect of $k_{H2O}/k_{D2O} = 1.40$ at 20 °C indicates that O–H/D bond cleavage is involved in the rate-determining step. Despite being more electron rich than **1**, $[Tp^*Ir(CO)_2]$ (**1***, Tp* = hydrotris(3,5-dimethylpyrazolyl)borate) reacts rapidly with adventitious water to give $[Tp^*Ir(CO_2H)(CO)H]$ (**2***). A proposed mechanism consistent with the relative reactivity of **1** and **1*** involves initial protonation of Ir(I) followed by nucleophilic attack on a carbonyl ligand. An X-ray crystal structure of **2*** shows dimer formation via pairwise H-bonding interactions of hydroxycarbonyl ligands (r(O···O) 2.65 Å). Complex **2*** is thermally stable but (like **2**) is amphoteric, undergoing dehydroxylation with acid to give $[Tp^*Ir(CO)_2H]^+$ (**3***) and decarboxylation with OH^- to give $[Tp^*Ir(CO)H_2]$ (**4***). Complex **2** undergoes thermal decarboxylation above ca. 50 °C to give $[TpIr(CO)H_2]$ (**4**) in a first-order process with activation parameters $\Delta H^{\ddagger} = 115\pm4$ kJ mol^{-1} and $\Delta S^{\ddagger} = 60\pm10$ J K^{-1} mol^{-1}.

Introduction

Metallocarboxylic acids, or hydroxycarbonyl complexes, are thought to be important intermediates in the reactions of transition metal carbonyls with water or hydroxide and were first proposed as intermediates in the oxidation of CO by Hg^{2+} ions in aqueous solution.[1] Species containing CO_2H ligands are thought to be involved in the water-gas shift (WGS) reaction, which occurs as a side reaction in the carbonylation of methanol to acetic acid catalyzed by rhodium (the Monsanto process) and iridium (the BP Cativa process).[2−7] Due to their propensity to undergo decarboxylation, relatively few hydroxycarbonyl complexes have been isolated and only a handful have been structurally characterized by X-ray crystallography.[8−16] The first hydroxycarbonyl complexes to be isolated were the iridium(III) complexes, $[IrCl_2(CO_2H)(CO)L_2]$ (L = PMe_2Ph, $AsMe_2Ph$) formed by reaction of $[IrCl_2(CO)_2L_2]^+$ with water.[17] Effects of ligand donor strength on the ease of formation and reactivity of hydroxycarbonyl species are well illustrated by the series of complexes $[CpFe(CO)LL']^+$ (L, L′ = CO, CO; CO, PPh_3; dppe).[18] The reaction of $[CpFe(CO)_3]^+$ with KOH results in rapid decomposition of the intermediate hydroxycarbonyl to give CO_2 and $[CpFe(CO)_2]_2$. By contrast, $[CpFe(CO)_2(PPh_3)]^+$ forms the stable $[CpFe(CO_2H)(CO)(PPh_3)]$, which

* To whom correspondence should be addressed. E-mail: a.haynes@sheffield.ac.uk.

† Current address: Department of Chemistry, University of York, Heslington, York, YO10 5DD, UK.

(1) Harkness, A. C.; Halpern, J. *J. Am. Chem. Soc.* **1961**, *83*, 1258.
(2) Cheng, C.-H.; Hendriksen, D. E.; Eisenberg, R. *J. Am. Chem. Soc.* **1977**, *99*, 2791.
(3) Baker, E. C.; Hendriksen, D. E.; Eisenberg, R. *J. Am. Chem. Soc.* **1980**, *102*, 1020.
(4) Singleton, T. C.; Park, L. J.; Price, J. L.; Forster, D. *Prepr. Div. Pet. Chem., Am. Chem. Soc.* **1979**, *24*, 329.
(5) Forster, D. *J. Chem. Soc., Dalton Trans.* **1979**, 1639.
(6) Sunley, G. J.; Watson, D. J. *Catal. Today* **2000**, *58*, 293.
(7) Haynes, A.; Maitlis, P. M.; Morris, G. E.; Sunley, G. J.; Adams, H.; Badger, P. W.; Bowers, C. M.; Cook, D. B.; Elliott, P. I. P.; Ghaffar, T.; Green, H.; Griffin, T. R.; Payne, M.; Pearson, J. M.; Taylor, M. J.; Vickers, P. W.; Watt, R. J. *J. Am. Chem. Soc.* **2004**, *126*, 2847.
(8) Balbach, B. K.; Helus, F.; Oberdorfer, F.; Ziegler, M. L. *Angew. Chem., Int. Ed. Engl.* **1981**, *20*, 470.
(9) Fujita, E.; Szalda, D. J.; Creutz, C.; Sutin, N. *J. Am. Chem. Soc.* **1988**, *110*, 4870.
(10) Bennett, M. A.; Robertson, G. B.; Rokicki, A.; Wickramasinghe, W. A. *J. Am. Chem. Soc.* **1988**, *110*, 7098.
(11) Mandal, S. K.; Ho, D. M.; Orchin, M. *J. Organomet. Chem.* **1992**, *439*, 53.
(12) Bennett, M. A., Jin, H, Willis, A. C. *J. Organomet. Chem.* **1993**, *451*, 249.
(13) Toyohara, K.; Nagao, H.; Adachi, T.; Yoshida, T.; Tanaka, K. *Chem. Lett.* **1996**, 27.
(14) Gibson, D. H.; Ding, Y.; Andino, J. G.; Mashuta, M. S.; Richardson, J. F. *Organometallics* **1998**, *17*, 5178.
(15) Gibson, D. H.; Sleadd, B. A.; Mashuta, M. S.; Richardson, J. F. *Acta Crystallogr., Sect. C: Cryst. Struct. Commun.* **1998**, *54*, 1584.
(16) Lee, D. W.; Jensen, C. M.; Morales-Morales, D. *Organometallics* **2003**, *22*, 4744.
(17) Deeming, A. J.; Shaw, B. L. *J. Chem. Soc. A* **1969**, 443.
(18) Grice, N.; Kao, S. C.; Pettit, R. *J. Am. Chem. Soc.* **1979**, *101*, 1627.

10.1021/ic0601844 CCC: $33.50
Published on Web 04/04/2006

Scheme 1

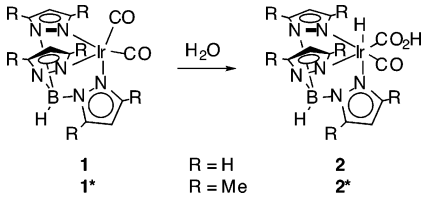

is deprotonated by a further equivalent of KOH to give the metallocarboxylate anion, $[CpFe(CO_2)(CO)(PPh_3)]^-$. The more electron rich $[CpFe(CO)(dppe)]^+$ fails to react with hydroxide due to the reduced electrophilicity of the carbonyl ligand.

Quantitative kinetic data for the formation and reactions of transition metal hydroxycarbonyl complexes are sparse. Ford and co-workers have reported kinetic data for the reactions of hydroxide with $[M(CO)_5]$ and $[M_3(CO)_{12}]$ to give $[M(CO)_4(CO_2H)]^-$ and $[M_3(CO)_{11}(CO_2H)]^-$, respectively (M = Fe, Ru, Os), along with the subsequent decarboxylations.[19,20] The iridium(I) dicarbonyl complexes, $[Tp'Ir(CO)_2]$ (**1**, Tp′ = Tp (hydrotris(pyrazolyl)borate); **1***, Tp′ = Tp* (hydrotris(3,5-dimethylpyrazolyl)borate)), have both previously been reported to react with water to give stable hydroxycarbonyl hydride complexes, $[Tp'Ir(CO_2H)(CO)H]$ (**2**, **2***), as shown in Scheme 1.[21,22] The two complexes exhibit notably different reactivity: Fernandez et al found that **1** reacts over several hours with water in acetonitrile to give **2**.[21] By contrast, Gutierrez-Puebla et al.[22] observed that the attempted synthesis of **1*** (by carbonylation of $[Tp^*Ir(C_2H_4)_2]$) actually gave **2***, attributed to a rapid reaction of **1*** with adventitious water.[23] In this paper, we report kinetic data for both the formation and decarboxylation of **2** and discuss the difference in reactivity between complexes with Tp and Tp* ligands. An X-ray crystal structure is presented for **2***.

Results and Discussion

Reactions of Water with $[Tp'Ir(CO)_2]$. In attempts to synthesize complex **1***, we have made analogous observations to those of Gutierrez-Puebla et al. Bubbling CO through a solution of $[Tp^*Ir(C_2H_4)_2]$ (in toluene, THF, or dichloromethane) initially gives some of the monocarbonyl, $[Tp^*Ir(C_2H_4)(CO)]$ (ν_{CO} 1990 cm^{-1}) which is then replaced by **2***. Small amounts of **1*** were detected (ν_{CO} 2035 and 1954 cm^{-1}) in toluene and THF, but the dicarbonyl complex could not be isolated. A communication by Ball et al. reported the reactivity of **1*** with acids, implying that isolation of this Ir(I) species is possible, but full synthetic details were not given.[24]

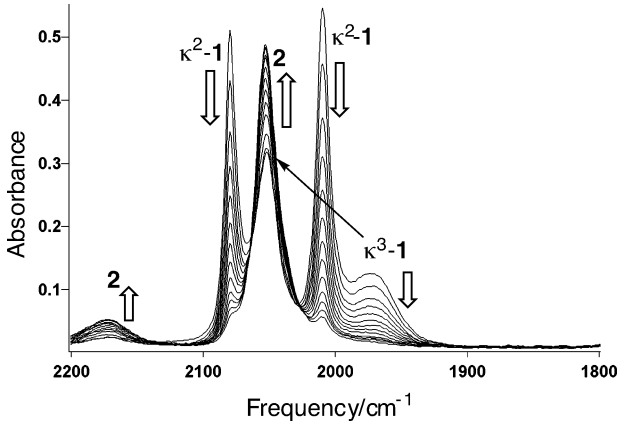

Figure 1. Series of IR spectra recorded during the reaction of **1** with water (2.78×10^{-3} mol dm^{-3}) in MeCN at 30 °C.

Table 1. IR Spectroscopic Data for Complexes **1**−**4** and **1***−**4*** in MeCN unless Otherwise Stated

complex	ν_{CO}/cm^{-1}	ν_{IrH}/cm^{-1}
$[TpIr(CO)_2]$ (**1**) (κ^2 isomer)	2080, 2010	
$[TpIr(CO)_2]$ (**1**) (κ^3 isomer)	2051, 1971	
$[Tp^*Ir(CO)_2]$ (**1***)	2035, 1954 [a]	
$[TpIr(CO_2H)(CO)H]$ (**2**)	2053, 1665	2175
$[Tp^*Ir(CO_2H)(CO)H]$ (**2***)	2046, 1661[b]	2174[b]
$[TpIr(CO)_2H]^+$ (**3**)[21]	2155, 2115	2165
$[Tp^*Ir(CO)_2H]^+$ (**3***)	2144, 2100[b]	2178[b]
$[TpIr(CO)H_2]$ (**4**)	2023	2171
$[Tp^*Ir(CO)H_2]$ (**4***)	2012	2164

[a] In toluene. [b] In CH_2Cl_2.

Scheme 2. κ^2-to-κ^3 Isomerism of **1** and Reaction with Water to Give **2**

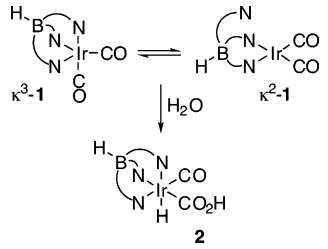

Kinetics of Reaction of 1 with Water. The reaction of **1** with water in MeCN can be conveniently monitored by infrared spectroscopy (Figure 1). At the start of the reaction, four terminal ν_{CO} bands are observed resulting from the presence of both κ^2 and κ^3 isomers of **1** (Table 1). During the course of the reaction, these bands all decay to be replaced by a single ν_{CO} band at 2053 cm^{-1} characteristic of **2** and almost coincident with the high-frequency band of the κ^3 reactant isomer. A weaker band grows at 2175 cm^{-1}, corresponding to the ν_{IrH} mode of **2**. When the reaction is carried out using D_2O, this band is not observed and the terminal ν_{CO} band shifts slightly to 2054 cm^{-1}. The low-frequency $\nu_{C=O}$ stretch for the hydroxycarbonyl ligand of **2** is obscured by the absorption of water in this region.

The observed reactivity is depicted in Scheme 2. During the reaction, the ν_{CO} bands for the κ^2 and κ^3 isomers of **1** decay in proportion to each other, indicating that the two species are in rapid equilibrium. The reaction kinetics were

(19) Gross, D. C.; Ford, P. C. *J. Am. Chem. Soc.* **1985**, *107*, 585.
(20) Trautman, R. J.; Gross, D. C.; Ford, P. C. *J. Am. Chem. Soc.* **1985**, *107*, 2355.
(21) Fernandez, M. J.; Rodriguez, M. J.; Oro, L. A. *J. Organomet. Chem.* **1992**, *438*, 337.
(22) Gutierrez-Puebla, E.; Monge, A.; Nicasio, M. C.; Perez, P. J.; Poveda, M. L.; Rey, L.; Ruiz, C.; Carmona, E. *Inorg. Chem.* **1998**, *37*, 4538.
(23) Similar reactivity toward adventitious water has recently been reported for a closely related tris(3,5-dimethylpyrazolyl)methane complex, $[(HCPz^*_3)Ir(CO)_2]^+$. Padilla-Martinéz, I. I.; Poveda, M. L.; Carmona, E. *Organometallics* **2002**, *21*, 93.
(24) Ball, R. G.; Ghosh, C. K.; Hoyano, J. K.; McMaster, A. D.; Graham, W. A. G. *J. Chem. Soc., Chem. Commun.* **1989**, 341.

analyzed by monitoring the decay of the 2010 cm^{-1} band of the κ^2 isomer. In the presence of excess water (pseudo-first-order conditions) an exponential decay shows the reaction to be first order in **1** (Figure S1, Supporting Information). The observed pseudo-first-order rate constants, k_{obs} (Table S1, Supporting Information), show a linear dependence on water concentration confirming the reaction to be first order in H_2O, following the rate law, $-d[\mathbf{1}]/dt = k[\mathbf{1}][H_2O]$. The slope of the plot of k_{obs} vs $[H_2O]$ gives a second-order rate constant of 1.65×10^{-4} dm^3 mol^{-1} s^{-1} at 25 °C. Measurements using D_2O allowed determination of a kinetic isotope effect of $k_{H2O}/k_{D2O} = 1.40$ at 20 °C. Variable-temperature kinetics for the reaction with H_2O were carried out between 15 and 35 °C. An Eyring plot (Figure S2, Supporting Information) gave activation parameters $\Delta H^{\ddagger} = 46 \pm 2$ kJ mol^{-1} and $\Delta S^{\ddagger} = -162 \pm 5$ J K^{-1} mol^{-1}. The moderate enthalpy of activation and relatively large negative entropy of activation suggest an associative transition state in the rate-determining step.

Fernandez et al. also reported that **1** reacts with MeOH and EtOH to give alkoxycarbonyls, $[TpIr(CO_2R)(CO)H]$ (R = Me, Et).[21] We carried out preliminary kinetic experiments on the reactions of **1** with alcohols but found that there was some deviation from clean pseudo-first-order behavior (possibly due to reaction with traces of water during the initial stages). Nevertheless, it was apparent from these measurements (at 20 °C, in MeCN/0.39 mol dm^{-3} ROH) that the order of reactivity is MeOH > EtOH > ^{i}PrOH with initial half-lives of ca. 15, 40, and 90 min, respectively.

Mechanism of Water Addition to [Tp′Ir(CO)$_2$]. Fernandez et al. ascribed the reactivity of **1** with water and alcohols[21] (and with primary amines[25]) to high electrophilicity of the terminal carbonyl ligands of **1**. However, nucleophilic attack on coordinated CO is more common for complexes with higher metal oxidation states or with electron deficient metal centers resulting from the coordination of several CO ligands. It is also notable that **1***, which contains the more strongly donating Tp* ligand, is even more reactive toward water than **1**. This is inconsistent with a mechanism involving direct nucleophilic attack by water on coordinated CO in the Ir(I) reactants.

We propose that nucleophilic attack on a CO ligand to generate a hydroxycarbonyl ligand occurs *after* oxidation of the Ir center from Ir(I) to Ir(III) by protonation. Nucleophilic attack by H_2O (or OH^-) would be expected to be much more facile for the cationic hydride species, $[Tp'Ir(CO)_2H]^+$ (**3′**) resulting from protonation. Initial protonation of the iridium center means that the reactivity will be mainly controlled by the basicity at this site, thereby explaining the higher reactivity of water with **1***. This mechanistic proposal also accounts for the observation that $[Tp^*Rh(CO)_2]$ does not react rapidly with adventitious water in the manner of its Ir analogue, **1***. The lower basicity of the Rh center means that protonation (by HBF_4) occurs instead on a pyrazolyl group of the Tp* ligand to give $[\kappa^2\text{-}\{HBPz^*_2(Pz^*H)\}Rh(CO)_2]^+$.[24]

Scheme 3. Proposed Mechanisms for the Reactions of **1** and **1*** with Water

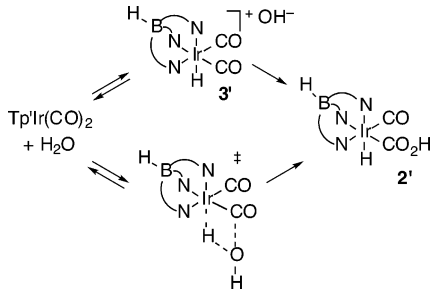

A mechanistic scheme for the reactions of **1** and **1*** with water is shown in Scheme 3. The upper pathway depicts the stepwise mechanism described above, in which the protonation step is probably a reversible pre-equilibrium. This mechanism is consistent with the kinetic isotope effect observed when H_2O was replaced by D_2O, since D_2O has a smaller self-ionization constant. For **1**, either the κ^2 or the κ^3 isomer of the reactant complex could, in principle, undergo protonation but the higher electron density bestowed on the Ir center by coordination of the third pyrazolyl group would probably make the κ^3 isomer more reactive. The lower part of Scheme 3 shows a closely related alternative route in which protonation of Ir and nucleophilic attack on CO occur in a concerted manner via a cyclic four-membered transition state. The stepwise and concerted routes are both consistent with the observed second-order kinetics. We favor the stepwise mechanism, however, since the cationic intermediates **3′** can be generated by protonation of **1′** with HBF_4 or by dehydroxylation of **2′**.[21,24]

The systems reported here represent an interesting contrast to others in the literature since coordination of stronger donor ligands usually inhibits CO activation by nucleophiles. For example, whereas $[IrCl_2(CO)_2(PPh_2Me)_2]^+$ reacts with a trace of water, $[IrCl_2(CO)(PPh_2Me)_3]^+$ is unreactive and only gives $[IrCl_2(CO_2H)(PPh_2Me)_3]$ on treatment with KOH.[26,27] A similar trend is shown by the $[CpFe(CO)LL']^+$ system (vide supra).[18] For $[Tp'Ir(CO)_2]$, however, the requirement for initial protonation to give an Ir(III) hydride means that higher reactivity toward water is displayed by the more electron rich Tp* complex.

It is appropriate to compare our observations with recent reports by Haskel and Keinan[28] and Reinartz et al.[29] concerning the reactivity of [TpPt(CO)Me] and [Tp*Pt(CO)Me]. Both complexes react with water to release CO_2 and give Pt(IV) dihydrides according to eq 1. In this case, however, it is the Tp complex which is more reactive, the Tp* complex requiring higher temperature and addition of KOH.

$$[Tp'Pt(CO)Me] + H_2O \rightarrow [Tp'PtH_2Me] + CO_2 \quad (1)$$

(25) Fernandez, M. J.; Modrego, J.; Rodriguez, M. J.; Santamaria, M. C.; Oro, L. A. *J. Organomet. Chem.* **1992**, *441*, 155.

(26) Bowman, K.; Deeming, A. J.; Proud, G. P. *J. Chem. Soc., Dalton Trans.* **1985**, 857.

(27) Deeming, A. J., Proud, G. P. *J. Organomet. Chem.* **1986**, *301*, 385.

(28) Haskel, A.; Keinan, E. *Organometallics* **1999**, *18*, 4677.

(29) Reinartz, S.; Baik, M.-H.; White, P. S.; Brookhart, M.; Templeton, J. L. *Inorg. Chem.* **2001**, *40*, 4726.

Table 2. Crystallographic Data for **2***

empirical formula	$C_{17}H_{24}BIrN_6O_3$
fw	563.43
space group	$P2_1/c$
a	14.0586(19) Å
b	7.8792(11) Å
c	20.815(3) Å
β	108.028(2)°
V	2192.5(5) Å^3
Z	4
T	150(2) K
λ	0.71073 Å
d_{calc}	1.707 g cm^{-3}
μ (Mo Kα)	6.118 mm^{-1}
R1 (wR2)	0.0491 (0.1281)
GOF on F^2	1.086

Table 3. Selected Bond Lengths (Å) and Bond Angles (deg) for **2***

Ir−C(1A)	1.734(16)	Ir−N(6)	2.163(6)
Ir−C(1B)	1.734(14)	O(2)−C(2)	1.349(11)
Ir−C(2)	1.989(9)	O(3A,B)−C(2)	1.245(11)
Ir−N(1)	2.131(7)	C(1A)−O(1A)	1.198(18)
Ir−N(3)	2.137(7)	C(1B)−O(1B)	1.169(16)
N(1)−Ir−N(3)	86.1(3)	C(1B)−Ir−N(6)	95.5(5)
N(1)−Ir−N(6)	85.4(3)	C(1A)−Ir−C(2)	86.8(8)
N(3)−Ir−N(6)	84.1(3)	C(1B)−Ir−C(2)	90.1(6)
C(2)−Ir−N(1)	90.4(3)	O(1A)−C(1A)−Ir	176(2)
C(2)−Ir−N(3)	90.8(4)	O(1B)−C(1B)−Ir	173.5(15)
C(2)−Ir−N(6)	173.6(3)	O(2)−C(2)−Ir	117.1(6)
C(1A)−Ir−N(1)	167.6(7)	O(3A)−C(2)−Ir	125.2(9)
C(1B)−Ir−N(1)	102.9(6)	O(3B)−C(2)−Ir	123.8(8)
C(1A)−Ir−N(3)	106.1(7)	O(3A)−C(2)−O(2)	113.8(10)
C(1B−Ir−N(3)	171.0(6)	O(3B)−C(2)−O(2)	117.2(9)
C(1A)−Ir−N(6)	98.2(8)		

The evidence supports direct nucleophilic attack by water on the Pt(II)-coordinated carbonyl ligand, rather than prior protonation to a Pt(IV) hydride.[30] The Pt(II) centers are significantly less electron rich than our Ir(I) systems (shown by ν(CO) 2087 and 2057 cm^{-1} for [TpPt(CO)Me] and [Tp*Pt(CO)Me], respectively), and protonation occurs at a pyrazolyl nitrogen in preference to the metal.[28,31] The inversion of relative reactivity toward water for Tp vs Tp* complexes can therefore be explained by the lower basicity of Pt(II) compared with Ir(I).

X-ray Crystal Structure of [Tp*Ir(CO$_2$H)(CO)H]. Crystals of **2*** suitable for an X-ray crystallographic structure determination were obtained. A summary of the crystallographic data is given in Table 2 with selected bond lengths and angles in Table 3. The molecular structure of **2*** is depicted in Figure 2. The coordination geometry surrounding the iridium center is a distorted octahedral arrangement with facial κ^3-coordination of the Tp* ligand. The three Ir−N bond distances are within the normal range for Tp*Ir complexes and are not distinguishable with statistical significance. The three N−Ir−N angles are all similar (ca. 85°) and within the expected range. Disorder is present between the terminal carbonyl and hydride ligands, and O(3) of the CO_2H ligand is also disordered. Each molecule of **2*** interacts with several neighboring molecules in the lattice to form a hydrogen-bonded network. The principal interaction is dimer formation

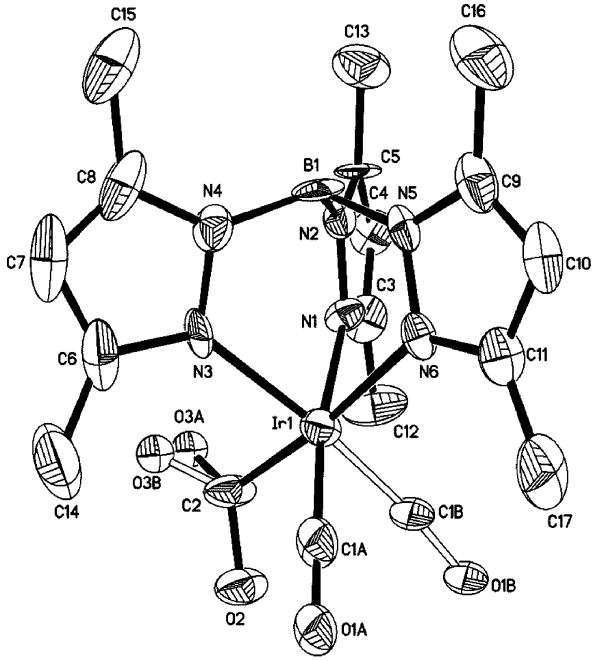

Figure 2. ORTEP drawing of **2***, showing disorder for C1O1 and O3. Thermal ellipsoids are shown at 50% probability, and hydrogen atoms are omitted for clarity.

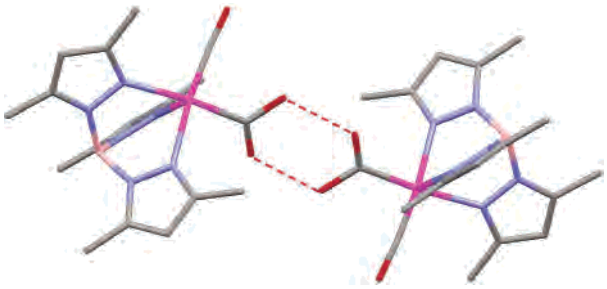

Figure 3. Intermolecular hydrogen-bonding interactions between hydroxycarbonyl ligands of **2***.

via pairwise hydrogen bonds between hydroxycarbonyl ligands of neighboring complexes (Figure 3). The intermolecular O···O distance (2.65 Å) is within the range for organic carboxylic acids[32] (e.g., 2.62 Å for the benzoic acid dimer in the solid state[33]). In addition to the pairwise hydrogen-bonding interactions between hydroxycarbonyl ligands, each molecule of **2*** forms subsidiary H-bonding interactions with four more neighboring molecules. These additional interactions occur between 5-methyl substituents of the Tp* pyrazolyl rings and oxygen atoms of CO or CO_2H ligands of neighboring molecules.

Of the nine other published X-ray structures of transition metal hydroxycarbonyl complexes[8−16] the only example containing iridium is [Ir(CO$_2$H)(κ^3-2,6-{CH$_2$P^{t}Bu$_2$}$_2$C$_6$H$_3$)H], which also displays pairwise intermolecular H-bonding between CO_2H ligands.[16] Similar dimer formation is also exhibited by *trans*-[Pt(CO$_2$H)(Ph)(PEt$_3$)$_2$],[10] [Pt(CO$_2$H)(κ^3-2,6-{CH$_2$PPh$_2$}$_2$C$_6$H$_3$)][12] and [Re(CO$_2$D)(CO)$_3$(dppp)]·C$_6$D$_6$.[11]

(30) Nucleophilic attack by RLi or NaHBEt$_3$ on the CO ligand of [Tp*Pt(CO)Me] has been demonstrated. Reinartz, S.; Brookhart, M.; Templeton, J. L. *Organometallics* **2002**, *21*, 247.

(31) Reinartz, S.; White, P. S.; Brookhart, M.; Templeton, J. L. *Organometallics* **2000**, *19*, 3854.

(32) Hadzi, D.; Detoni, S. In *The Chemistry of Functional Groups; Supplement B: The Chemistry of Acid Derivatives*; Patai, S., Ed.; John Wiley and Sons: Chichester, 1979; pp 214−266.

(33) Wilson, C. C.; Shankland, N.; J, F. A. *J. Chem. Soc., Faraday Trans.* **1996**, 5051.

Scheme 4. Acid/Base Reactivity of **2***

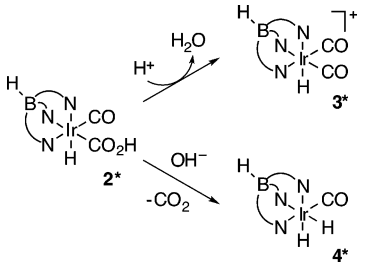

Scheme 5. Thermal Decarboxylation of **2**

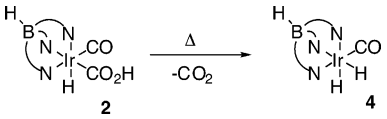

The intermolecular distance between H-bond donor and acceptor oxygen atoms is slightly smaller for the two Ir(III) complexes than for the Pt(II) and Re(I) examples, perhaps reflecting the strength of the H-bonding attraction. The Ir−CO_2H bond length is shorter (1.985(8) Å) in **2*** than in [Ir(CO_2H)(κ^3-2,6-{$CH_2P^tBu_2$}$_2C_6H_3$)H] (2.10(2) Å), probably due to the smaller trans influence of a pyrazolyl relative to an aryl donor.

Interestingly, the cationic ruthenium complexes [Ru(CO_2H)(CO)(phen)$_2$]PF_6[14] and [Ru(CO_2H)(CO)(bipy)-(κ^2-terpy)]PF_6[15] exist as monomers in the solid state. In the first case, a H-bonding interaction exists between the CO_2H ligand and a PF_6^- counterion and the packing is also influenced by intermolecular π-stacking of the phen ligands. In the second example, there is an intramolecular H-bond between the CO_2H ligand and the uncoordinated pyridyl nitrogen of the κ^2-terpyridine ligand, which forces the CO_2H ligand to adopt a syn instead of the normal anti conformation. A third cationic Ru(II) complex, [Ru(CO_2H)(CO)(bipy)$_2$]-CF_3SO_3, has an expanded dimeric structure in which H-bonding between the hydroxycarbonyl ligands is mediated by bridging water molecules.[13] Thus, only the *neutral* hydroxycarbonyl complexes display dimerization by simple pairwise H-bonding in the solid state. Electrostatic repulsion between cationic complexes may contribute to this observation, but competitive H-bonding to anions and solvent molecules (and in one case π-stacking) seem also to be important in determining the packing structure.[34]

Acid/Base Reactivity of [Tp*Ir(CO_2H)(CO)H] (2*). Fernandez et al. showed that, like many transitional metal hydroxycarbonyl complexes, [TpIr(CO_2H)(CO)H] (**2**) is amphoteric.[21] Treatment with strong acid (HBF_4) resulted in dehydroxylation to give [TpIr(CO)$_2$H]$^+$ (**3**), whereas treatment with strong base (KOH) led to decarboxylation, giving the dihydride, [TpIr(CO)H_2] (**4**). We found very similar behavior for the Tp* system in reactions carried out on a spectroscopic scale. Thus, the reaction of **2*** with [(CF_3SO_2)$_2$N]H in CH_2Cl_2 results in dehydroxylation to give the known[24] cationic iridium(III) hydride, [Tp*Ir(CO)$_2$H]$^+$ (**3***; δ ^{1}H −15.87, Ir*H*; IR data in Table 1). Complex **2*** fails to react with moderate bases such as NEt_3 but reacts with Bu_4NOH in MeCN to undergo decarboxylation, giving the known[22] monocarbonyl dihydride, [Tp*Ir(CO)H_2] (**4***, δ ^{1}H −16.01, IrH_2; IR data in Table 1). The reactions of **2*** with acid and base are illustrated in Scheme 4.

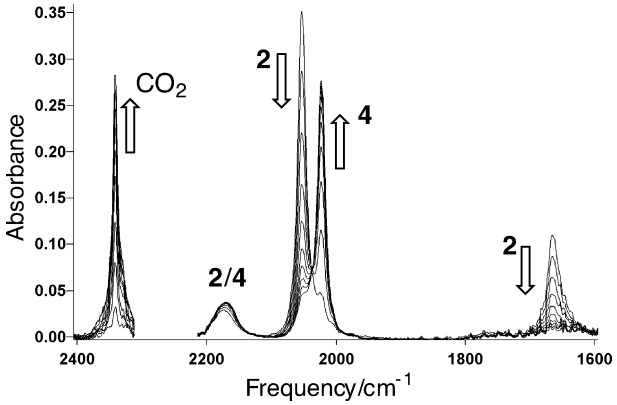

Figure 4. Series of IR spectra recorded during the thermal decarboxylation of **2** in MeCN at 56 °C (region between 2310 and 2220 cm^{-1} masked by strong solvent ν_{CN} absorption).

Thermal Decarboxylation of [Tp′Ir(CO_2H)(CO)H] (2). Fernandez et al. reported that **2** undergoes decarboxylation in refluxing acetonitrile to give [TpIr(CO)H_2] (**4**) (Scheme 5).[21] We have monitored the kinetics of this thermal reaction at temperatures between 50 and 70 °C using IR spectroscopy. During the course of the reaction, bands for the terminal carbonyl and hydroxycarbonyl ligands of **2** (2053 and 1665 cm^{-1}, respectively) decay and a new terminal ν_{CO} band appears at 2023 cm^{-1} for **4**, as shown in Figure 4. At the same time, the ν_{IrH} for **2** at 2175 cm^{-1} shifts to 2171 cm^{-1} for **4** and an intense band grows at 2342 cm^{-1}, characteristic of dissolved CO_2.

Plots of absorbance versus time show that the terminal carbonyl band of **2** at 2053 cm^{-1} decays exponentially (Figure S3, Supporting Information), indicating that the reaction is first order in **2**. Observed rate constants are given in the Supporting Information (Table S2), and an Eyring plot gave activation parameters $\Delta H^{\ddagger} = 115 \pm 4$ kJ mol^{-1} and $\Delta S^{\ddagger} = 60 \pm 10$ J K^{-1} mol^{-1}. The relatively high enthalpy of activation and moderate positive entropy of activation are indicative of a dissociative transition state. The Tp* analogue **2*** is more robust, and only slight decomposition (accompanied by formation of a small amount of CO_2) was observed at 70 °C in MeCN.

Very few kinetic studies involving decarboxylation of transition metal hydroxycarbonyl complexes have been reported. Katz et al.[35] studied the pH-dependent kinetics for the decomposition of [Co(en)$_2$(OH_2)(CO_2H)]$^{2+}$ (en = ethylenediamine) at 298 K, while Ford and co-workers monitored the kinetics of formation of [M(CO)$_4$H] and [M$_3$(CO)$_{11}$H]$^-$ during the reactions of hydroxide with [M(CO)$_5$] and [M$_3$(CO)$_{12}$] (M = Fe, Ru, Os).[19,20] Catellani

(34) The two other structurally characterized hydroxycarbonyl complexes contain CO_2H ligands bridging either two Co centers (Fujita, E.; Szalda, D. J.; Creutz, C.; Sutin, N. *J. Am. Chem. Soc.* **1988**, *110*, 4870) or three Re centers (Balbach, B. K.; Helus, F.; Oberdorfer, F.; Ziegler, M. L. *Angew. Chem., Int. Ed. Engl.* **1981**, *20*, 470).

(35) Katz, N. E.; Szalda, D. J.; Chou, M. H.; Creutz, C.; Sutin, N. *J. Am. Chem. Soc.* **1989**, *111*, 6591.

Scheme 6. Possible Routes in the Elimination of CO_2 from **2** during Thermal Decarboxylation

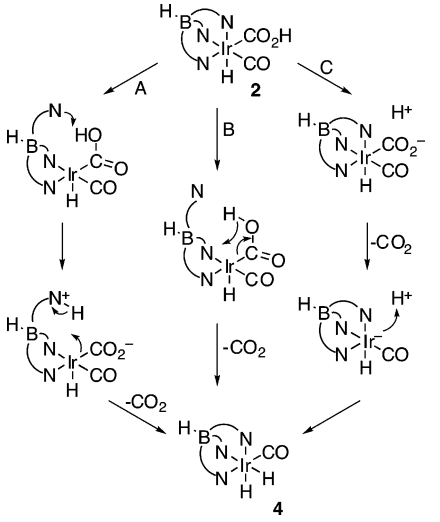

and Halpern mentioned in a communication[36] their intention to study the kinetics of decarboxylation of $[Pt(CO_2H)Cl(PEt_3)_2]$, but no such data have apparently been published. To our knowledge, our activation parameters for decarboxylation of **2** are the first for this class of reaction.

Three possible mechanisms for the thermal decarboxylation of **2** are presented in Scheme 6. The positive entropy of activation is indicative of a dissociative transition state. Paths A and B involve dechelation of one of the pyrazolyl arms of the Tp ligand to give a vacant coordination site. In path A, this is followed by intramolecular proton transfer from the hydroxycarbonyl ligand to the pendant pyrazolyl group. Decarboxylation then occurs with transfer of the proton to the metal and re-coordination of the pendant pyrazolyl arm to give the product, **4**. In path B, the pendant pyrazolyl arm remains a spectator while decarboxylation occurs via concerted β-hydride transfer to the metal (as suggested for related reactions[18]). Path C involves ionization of the metallocarboxylic acid followed by elimination of CO_2 to give an anionic iridium(I) intermediate which is protonated to yield **4**. These pathways are difficult to distinguish experimentally, but dechelation of one of the pyrazolyl rings is plausible since $\kappa^3-\kappa^2$ isomerization has been shown to be important in other reactions of tris(pyrazolyl)borate complexes, such as C−H activation[37−41] and protonation or methylation at the metal center.[42−45] While there is no direct evidence that a pendant pyrazolyl group acts as a transient proton acceptor, as suggested in path A, the observed[24] protonation of a pyrazolyl nitrogen in $[Tp^*Rh(CO)_2]$ indicates the feasibility of such a mechanism. Another potential mechanism (not illustrated) could proceed via a β-elimination in a 16-electron intermediate formed by dissociation of CO.

The Tp′Ir systems studied here can be considered to model important steps in the Rh- or Ir (+iodide)-catalyzed WGS reactions which occur in parallel to homogeneous catalytic methanol carbonylation under acidic conditions. In those cases, the M(III) iodocarbonyl species $[M(CO)_2I_4]^-$ and $[M(CO)_3I_3]$ (arising via $[M(CO)_2I_3H]^-$ from oxidation of $[M(CO)_2I_2]^-$ by HI) are thought to undergo nucleophilic attack by water, [2−7] but the presumed hydroxycarbonyl intermediates (e.g., $[M(CO_2H)(CO)_2I_3]^-$) have not been detected. Tris(pyrazolyl)borate ligands have a strong stabilizing influence, enabling isolation of the hydroxycarbonyl species **2** and **2*** and dihydrides **4** and **4***. In principle, a catalytic WGS cycle based on $[Tp'Ir(CO)_2]$ could be closed by displacement of H_2 from $[Tp'Ir(CO)H_2]$ by CO. However, Fernandez et al. found that complex **4** fails to react with CO in refluxing THF,[21] showing that reductive elimination of H_2 is not facile.

Summary

Kinetic measurements on the oxidative addition of water to **1** show the reaction to be second order with a kinetic isotope effect, $k_{H2O}/k_{D2O} = 1.4$. The low reactivity of the Tp complex **1** relative to its Tp* analogue **1*** is interpreted in terms of a mechanism involving initial protonation at Ir(I) followed by nucleophilic attack on a carbonyl ligand in the cation $[Tp'Ir(CO)_2H]^+$. An X-ray crystal structure of $[Tp^*Ir(CO_2H)(CO)H]$ (**2***) represents only the 10th structurally characterized example of a hydroxycarbonyl complex. The solid-state structure consists of dimers held together by pairwise H-bonding interactions between CO_2H ligands, as well as a network of subsidiary H-bonds. Kinetic studies of the thermal decarboxylation of $[TpIr(CO_2H)(CO)H]$ (**2**) gave activation parameters indicative of a dissociative mechanism, and routes involving dechelation of a pyrazolyl arm of the Tp ligand are proposed.

Experimental Section

General. Infrared solution spectra were recorded on a Mattson Genesis FTIR spectrometer using a CaF_2 cell (path length 0.5 mm). ^1H NMR spectra were recorded on a Bruker AC250 instrument in pulsed Fourier transform mode, fitted with a Bruker B ACS-60 sample changer and using solvent as internal reference.

Synthetic Procedures. Synthetic procedures were carried out under N_2 using standard Schlenk techniques. $[TpIr(CO)_2]$ (**1**),[46] $[TpIr(CO_2H)(CO)H]$ (**2**),[21] and $[Tp^*Ir(C_2H_4)]$[47] were prepared by literature methods. Reagents were used as supplied. Solvents were

(36) Catellani, M.; Halpern, J. *Inorg. Chem.* **1980**, *19*, 566.
(37) Bloyce, P. E.; Mascetti, J.; Rest, A. J. *J. Organomet. Chem.* **1993**, *444*, 223.
(38) Bromberg, S. E.; Yang, H.; Asplund, M. C.; Lian, T.; McNamara, B. K.; Kotz, K. T.; Yeston, J. S.; Wilkens, M.; Frei, H.; Bergman, R. G.; Harris, C. B. *Science* **1997**, *278*, 260.
(39) Wick, D. D.; Goldberg, K. I. *J. Am. Chem. Soc.* **1997**, *119*, 10235.
(40) Wick, D. D.; Reynolds, K. A.; Jones, W. D. *J. Am. Chem. Soc.* **1999**, *121*, 3974.
(41) Jensen, M. P.; Wick, D. D.; Reinartz, S.; White, P. S.; Templeton, J. L.; Goldberg, K. I. *J. Am. Chem. Soc.* **2003**, 8614.
(42) Canty, A. J.; Dedieu, A.; Jin, H.; Milet, A.; Richmond, M. K. *Organometallics* **1996**, *15*, 2845.
(43) O'Reilly, S. A.; White, P. S.; Templeton, J. L. *J. Am. Chem. Soc.* **1996**, *118*, 5684.
(44) Reinartz, S.; Brookhart, M.; Templeton, J. L. *Organometallics* **2002**, *21*, 247.
(45) Chauby, V.; Daran, J.-C.; Serra-Le Berre, C.; Malbosc, F.; Kalck, P.; Gonzalez, O. D.; Haslam, C. E.; Haynes, A. *Inorg. Chem.* **2002**, *41*, 3280.
(46) Tanke, R. S.; Crabtree, R. H. *Inorg. Chem.* **1989**, *28*, 3444.
(47) Alvarado, Y.; Boutry, O.; Gutierrez, E.; Monge, A.; Nicasio, M. C.; Poveda, M. L.; Perez, P. J.; Ruiz, C.; Bianchini, C.; Carmona, E. *Chem. Eur. J.* **1997**, *3*, 860.

dried by distillation immediately prior to use. THF was dried over 3 Å molecular sieves before distillation over sodium and benzophenone. Acetonitrile, dichloromethane, and toluene were distilled over calcium hydride.

[Tp*Ir(CO$_2$H)(CO)H] (2*).[22] [Tp*Ir(C$_2$H$_4$)$_2$] (50 mg, 0.10 mmol) was dissolved in the CH_2Cl_2 (10 cm^3), and CO bubbled through the pale yellow solution at room temperature. The reaction was monitored using infrared spectroscopy, which showed that [Tp*Ir(CO)(C$_2$H$_4$)] (ν_{CO} 1990 cm^{-1}) was formed initially. After the mixture was stirred for 24 h, bands at 2174, 2046, and 1661 cm^{-1} were observed, corresponding to the formation of [Tp*Ir(CO$_2$H)(CO)H]. The solvent was removed in vacuo, and recrystallization from dichloromethane afforded the product as colorless needlelike crystals; yield 39 mg (70%). A suitable crystal was selected for an X-ray crystallographic study. Anal. Calcd for $C_{17}H_{24}IrBN_6O_3$: C, 36.23; H, 4.30; N, 14.92. Found: C, 36.15; H, 4.16; N, 14.98. IR (CH_2Cl_2): ν_{IrH} 2174 cm^{-1}; ν_{CO} 2046 and 1661 cm^{-1}. NMR ($CDCl_3$): δ ^{1}H: 5.90, 5.85, 5.80 (each 1H, s, C−H), 2.40, 2.35, 2.32, 2.28, 2.26, 2.20 (each 3H, s, CH_3) in agreement with literature data.[22]

Reaction of 2* with (CF$_3$SO$_2$)$_2$NH. This reaction was performed on a spectroscopic scale. Complex **2*** (2 mg) was dissolved in CH_2Cl_2 (2 cm^3) to which was added dropwise a solution of $(CF_3SO_2)_2NH$ (10 mg) in CH_2Cl_2 (5 cm^3). Regular monitoring by IR spectroscopy indicated replacement of bands for **2*** by those of [Tp*Ir(CO)$_2$H]$^+$ (**3***)[24] (ν_{IrH} 2178 cm^{-1}, ν_{CO} 2100, 2044 cm^{-1}). NMR: δ ^{1}H −15.87 (IrH).

Reaction of 2* with Bu$_4$NOH. This reaction was performed on a spectroscopic scale. Complex **2*** (2 mg) was dissolved in MeCN (2 cm^3), and a solution of methanolic Bu$_4$NOH (1 cm^3, 1 mol dm^{-3}) made up to 10 cm^3 in MeCN was added dropwise. Regular monitoring by IR spectroscopy indicated replacement of bands for **2*** by those of [Tp*Ir (CO)H$_2$] (**4***)[22] (ν_{IrH} 2164 cm^{-1}, ν_{CO} 2012 cm^{-1}). NMR: δ ^{1}H −16.01 (IrH$_2$).

Kinetic Measurements. Reaction monitoring was achieved using a Mattson Genesis FTIR spectrometer (2 cm^{-1} resolution). For the reaction of water with complex **1**, a solution of water in MeCN of the desired concentration was prepared in a 5 cm^3 graduated flask. A portion of this solution was used to record a background spectrum. Another portion (typically 1000 μL) was added to the solid Ir complex (2 mg) in a sample vial to give a reaction solution containing ca. 4 mmol dm^{-3} [Ir]. Pseudo-first-order conditions were employed, with at least a 100-fold excess of H_2O, relative to [Ir]. A portion of the reaction solution was quickly transferred to the IR cell, and data collection was started. The IR cell (0.5 mm path length, CaF_2 windows) was maintained at constant temperature by a thermostated jacket. Spectra (2400−1600 cm^{-1}) were scanned and saved at regular time intervals under computer control. An analogous procedure was used for the thermal decarboxylation of **2**, using neat MeCN as the reaction solvent. Absorbance vs time data for the appropriate ν_{CO} bands were extracted and analyzed off-line using Kaleidagraph curve-fitting software. For each experiment, the decay of the appropriate ν_{CO} band was fitted to an exponential curve, with correlation coefficient ≥0.999, to give a pseudo-first-order rate constant. Each kinetic run was repeated at least twice to check reproducibility, the k_{obs} data reported being averaged values.

X-ray Crystal Structure of [Tp*Ir(CO$_2$H)(CO)H] (2*). Data collected were measured on a Bruker Smart CCD area detector with Oxford Cryosystems low-temperature system. Cell parameters were refined from the setting angles of 550 reflections (θ range 1.52° < 28.39°). Reflections were measured from a hemisphere of data collected of frames each covering 0.3° in Ω. Of the 12 319 reflections measured, all of which were corrected for Lorentz and polarization effects and for absorption by semiempirical methods based on symmetry-equivalent and repeated reflections (minimum and maximum transmission coefficients 0.3100 and 0.5272), 3298 independent reflections exceeded the significance level $|F|/\sigma(|F|) > 4.0$. The structure was solved by direct methods and refined by full matrix least-squares methods on F^2. Hydrogen atoms were placed geometrically and refined with a riding model (including torsional freedom for methyl groups) and with U_{iso} constrained to be 1.2 (1.5 for methyl groups) times U_{eq} of the carrier atom. Refinement converged at a final R = 0.0491 (wR2 = 0.1281, for all 4279 data, 280 parameters, mean and maximum δ/σ 0.000, 0.001) with allowance for the thermal anisotropy of all non-hydrogen atoms, with the exception of O3 which was found to be disordered and refined to an occupancy of 56:44 and the carbonyl C1,O1 which was also found to be disordered and refined to an occupancy of 56:44. Minimum and maximum final electron density −1.961 and 1.833 e·Å^{-3}. A weighting scheme $w = 1/[\sigma^2(F_o^2) + (0.0642P)^2 + 0.00P]$ where $P = (F_o^2 + 2F_c^2)/3$ was used in the latter stages of refinement. Complex scattering factors were taken from the program package SHELXTL[48] as implemented on the Viglen Pentium computer.

Acknowledgment. We thank the EPSRC and BP Chemicals Ltd. for funding this research (studentships to P.I.P.E. and C.E.H). We also thank Dr. David Law, Dr. Glenn Sunley, Dr. Lee Brammer, and Mr. Harry Adams for helpful discussions and Mr. Sam Hawxwell for conducting some preliminary studies.

Supporting Information Available: Kinetic data and plots for the reaction of water with **1** and decarboxylation of **2** and crystallographic information file (CIF) for **2***. This material is available free of charge via the Internet at http://pubs.acs.org.

IC0601844

(48) Sheldrick, G. M. *SHELXTL, An integrated system for solving and refining crystal structures from diffraction data*, revision 5.1; Bruker AXS Ltd: Madison, WI.